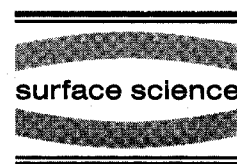




ELSEVIER

Surface Science 360 (1996) 55–60



# Hydrogen-induced missing-row reconstructions of Pd(110) studied by scanning tunneling microscopy

Elisabeth Kampshoff \*, Nicolas Waelchli, Alexander Menck, Klaus Kern

*Institut de Physique Expérimentale, EPFL, CH-1015 Lausanne, Switzerland*

Received 2 January 1996; accepted for publication 1 March 1996

## Abstract

The effect of hydrogen adsorption on the Pd(110) surface structure at room temperature has been studied by scanning tunneling microscopy. Depending on the partial pressure of hydrogen two different reconstructions of Pd(110) have been observed: a  $(1 \times 3)$  phase at hydrogen pressures in the  $10^{-9}$  mbar range and an additional  $(1 \times 2)$  phase at  $p_{\text{H}_2} \geq 5 \times 10^{-8}$  mbar. Both reconstructions are found to be of the missing-row type. The evolution of the surface reconstructions has been followed in situ.

**Keywords:** Hydrogen; Palladium; Scanning tunneling microscopy; Surface reconstruction; Surface structure, morphology

## 1. Introduction

It is a well known phenomenon that the interaction of adsorbates with a metal surface may lead to a complete restructuring of the surface with the number of discovered adsorbate–substrate systems undergoing this reconstruction process raising from year to year [1]. Molecules like sulphur, oxygen, carbon and nitrogen interact strongly with the substrate so that surface rearrangements in order to minimize the total surface free energy seem quite reasonable. Weakly chemisorbed species like hydrogen can also induce the restructuring if the surface has an inherent tendency towards reconstruction. Examples are the (110) surfaces of the 3d and 4d metals Ni and Pd. While the 5d homologue Pt has a missing-row reconstructed ground state, the unreconstructed  $(1 \times 1)$  structure is more stable in the 3d and 4d metals. A small

charge redistribution due to the chemisorption of hydrogen is however sufficient to induce a reconstruction of the Ni(110) and the Pd(110) surface [2–5]. In the temperature range between 120 K  $< T < 300$  K two different kinds of  $(1 \times 2)$  reconstructions have been found on both substrates, one a low temperature pairing-row, and two a missing-row/added-row reconstruction.

In this paper we will represent the results of our STM measurements on the system H/Pd(110). This system is of technical relevance as an example for hydrogen storage due to its high solubility in the Pd bulk [6–10]. Different structures of the H/Pd(110) surface as a function of temperature and hydrogen coverage have already been examined [2,3]. In the low temperature regime below 200 K and in the submonolayer hydrogen coverage range the adsorbed gas can be described as a disordered lattice gas. Ordering to a  $(2 \times 1)$  superstructure sets in at  $\theta_{\text{H}} = 1$  ML, the saturation coverage of hydrogen on the unreconstructed

\* Corresponding author. Fax: +41 21 693 3604.

Pd(110) surface. With increasing hydrogen exposure the sharp ( $2 \times 1$ ) LEED pattern loses intensity in favour to a ( $1 \times 2$ ) superstructure which is most pronounced at  $\theta_{\text{H}} = 1.5$  ML. The Pd(110) surface is found to be restructured into paired rows with the additional 0.5 ML hydrogen atoms adsorbing in-between. At an annealing temperature of 200 K these hydrogen atoms dissolve into the bulk, the ( $1 \times 2$ ) reconstruction gets lifted and the ( $2 \times 1$ ) superstructure reappears. Above 250 K another ( $1 \times 2$ ) superstructure is revealed which is assigned to a missing-row/added-row reconstruction of the surface induced by the adsorption of one monolayer hydrogen [2]. Due to the fair amount of disorder along [001] the LEED pattern of this structure appears streaky.

Our STM measurements reveal the existence of an additional phase in the H/Pd(110) phase diagram. At 300 K and hydrogen coverages between  $0.3 \text{ ML} < \theta_{\text{H}} < 0.5 \text{ ML}$  a ( $1 \times 3$ ) missing-row reconstruction has been found. Upon increasing the hydrogen coverage to 0.8 ML a coexistence regime with ( $1 \times 3$ ) and ( $1 \times 2$ ) phases is observed before the surface completely transfers to a ( $1 \times 2$ ) reconstruction close to monolayer completion. The stability of these phases was checked by annealing experiments. At 350 K the Pd(110) surface is found to relax back into the stable ( $1 \times 1$ ) surface.

## 2. Experimental

The experiments were carried out in an UHV chamber described in detail in Ref. [11]. The STM is a beetle type STM designed for measurements in the temperature range between 150 and 600 K. All STM images are taken in the constant current mode with tunneling currents  $< 2 \text{ nA}$  and a tip to surface voltage of 2 V. The vacuum chamber is equipped with standard facilities for surface preparation and surface quality control. The Pd(110) single crystal surface was cleaned by several cycles of Argon sputtering at 700 K, annealing in an oxygen atmosphere at 600 K and flash annealing to 900 K. This procedure resulted in sharp ( $1 \times 1$ ) LEED patterns. The Auger spectra showed no contamination. The Pd(110) surface was exposed to hydrogen at 300 K. By backfilling the chamber

via a standard leak valve the partial pressure of hydrogen was fixed and in situ STM measurements were performed as a function of exposure time. The recording of a single STM image took about 2 min.

## 3. Results and discussion

Fig. 1 shows a series of STM images characterizing the morphology of the Pd(110) surface during the adsorption process of hydrogen at 300 K. The  $\text{H}_2$  partial pressure was fixed to  $2 \times 10^{-9}$  mbar. The hydrogen uptake behavior of the Pd(110) surface can be separated into two regimes. In the first stage of hydrogen exposure a kinetic equilibrium between the adsorption of hydrogen, its diffusion into the Pd bulk and the desorption will be established. The change in surface morphology during this stage is shown in the STM images in Fig. 1a and b. The uppermost STM image was taken 45 min after starting the hydrogen exposure. As a result of hydrogen exposure we see the formation of holes in the Pd substrate as well as adatom islands on the terraces. Both, the adatom as well as the vacancy islands are elongated in the close packed  $[\bar{1}10]$  direction of the substrate. Their form nicely reflects the anisotropy of the (110) surface with respect to diffusion and nucleation [12]. With increasing exposure the number of vacancy and adatom islands increases continuously as shown in Fig. 1b.

The height of the adislands and the depth of the vacancy islands corresponds to the height of a monoatomic Pd(110) step. It is thus natural to conclude that the adislands have nucleated from Pd-adatoms which have been kicked out of the surface. The vacancy islands on the other hand are the result of a nucleation and growth process of the corresponding monovacancies. Surprisingly, the total length of vacancy and adislands on large terraces differs by a factor of 2, i.e. the total hole length is twice as large as the adisland length. This result implies that the Pd vacancy islands are monoatomic in width whereas the adislands consist of Pd dimer chains. Our experiments of homoepitaxial Pd/Pd(110) growth confirm this result [13]. At a deposition temperature of 300 K the shape of

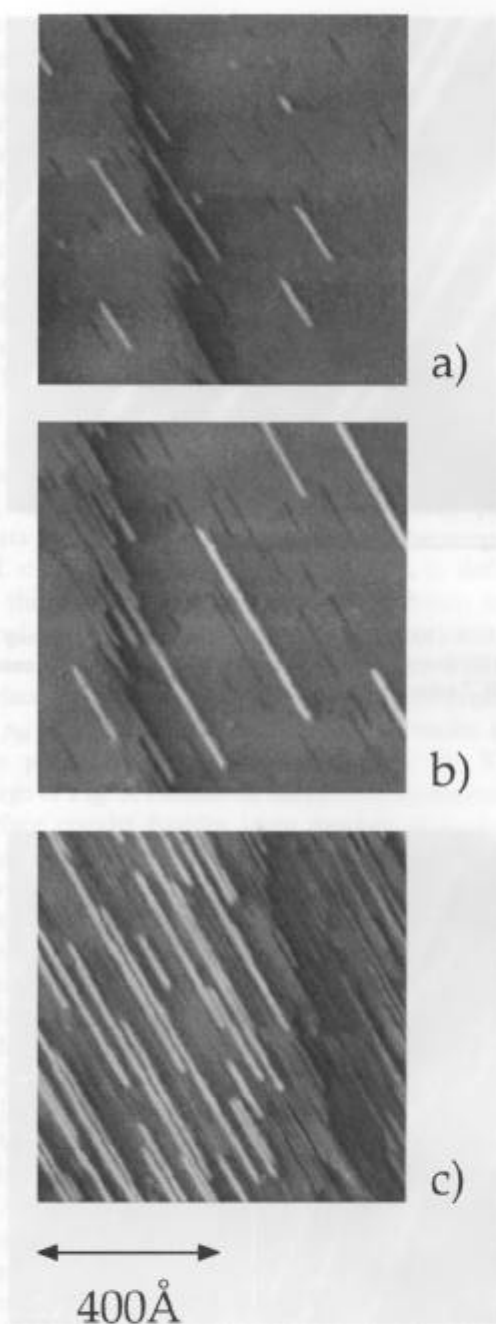


Fig. 1. Morphology of the Pd(110) surface during hydrogen exposure. The STM images are taken after (a) 45 min, (b) 95 min and (c) 300 min of hydrogen exposure at 300 K with a fixed pressure of  $p_{\text{H}_2} = 2 \times 10^{-9}$  mbar.

the grown Pd adislands is kinetically determined. In the Pd coverage range below 0.2 ML they consist also of dimer chains oriented along the closed packed  $[\bar{1}10]$  direction.

What is the origin of the vacancy and the adatom islands? The high solubility of hydrogen into the Pd bulk is well known [6–10] and we assume that the formation of vacancy and adatom islands is associated with the diffusion of hydrogen onto subsurface sites and into the Pd bulk. The scenario shown in the STM images of Fig. 1a and b can be rationalized as follows: the hydrogen atoms are adsorbed on the Pd substrate on sites with almost threefold coordination [8]. In order to establish the equilibrium between adsorbed and subsurface hydrogen some H atoms have to open up their way into the Pd bulk. The most favourable subsurface adsorption geometry in the fcc lattice is the octahedral site [6,8]. In order to reach this site the hydrogen atom has to penetrate the topmost Pd layer in the  $[\bar{1}\bar{1}\bar{1}]$  direction. Due to the instability of the (110) surface, the Pd atom from the topmost layer is kicked out and replaced by the hydrogen atom. The H atom is now surrounded by the densely packed (111) facets of the Pd crystal and subsequent diffusion into the Pd bulk can be achieved via interstitial sites. The kicked out Pd atoms nucleate on the large terraces and some of them may also reach the step edges. Compared to direct hydrogen attack at step edges, this process is much less probable. Taking into account the high density of Pd rows growing from the edge as well as their regular arrangement (see Fig. 1b) it seems likely that the main part of adatom rows growing from step edges are due to the direct hydrogen attack.

At the very beginning of the hydrogen exposure the coverage of Pd adatoms is proportional to the hydrogen exposure (Fig. 2). Measurements with different hydrogen partial pressures reveal a proportionality factor  $m = 0.0039 \text{ ML langmuir}^{-1}$ . Considering our simple model this amount of Pd adatoms is equal to the minimum amount of hydrogen atoms located in the subsurface region. It is remarkable here that within the experimental error the graph of Fig. 2 intersects the origin. This result implies that there is no critical hydrogen exposure needed to initiate the morphology

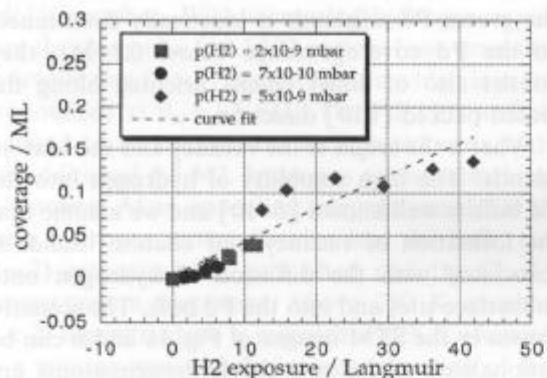


Fig. 2. Pd adatom coverage as a function of hydrogen exposure at 300 K (■  $2 \times 10^{-9}$  mbar, ◆  $5 \times 10^{-9}$  mbar and ●  $7 \times 10^{-10}$  mbar).

changes of the Pd(110) surface. Our experiments indicate that the hydrogen adsorption is not completed instantaneously but covers the whole timescale shown in the graph of Fig. 2. Conrad and co-workers have shown that the adsorption/desorption equilibrium is coupled to the bulk diffusion and that relatively long periods are necessary until at a fixed hydrogen partial pressure also a stationary state of surface coverage is reached [14]. At hydrogen partial pressures  $\leq 5 \times 10^{-9}$  mbar our experiments reveal a time scale of several hours.

At a critical hydrogen exposure above  $\sim 30$  L the second stage in the restructuring of the surface sets in. This stage involves a substantial mass transport going in hand with a pronounced change in the surface morphology (Fig. 1c). The amount of missing rows in the surface drastically increases and they start to order laterally. Fig. 3 shows a  $400 \text{ \AA} \times 400 \text{ \AA}$  zoom-in of Fig. 1c revealing local ordering of the missing rows in a  $(1 \times 3)$  superlattice. A fair amount of disorder, however, is still present at the surface. This is consistent with the corresponding LEED measurements showing a very streaky  $(1 \times 3)$  pattern. A further exposure to the hydrogen atmosphere substantially improves the order of the missing row reconstruction. This is demonstrated in Fig. 4. The entire surface exhibits a perfect  $(1 \times 3)$  ordering which gives rise to a very sharp LEED pattern. This final transformation into the well ordered  $(1 \times 3)$  missing-row phase

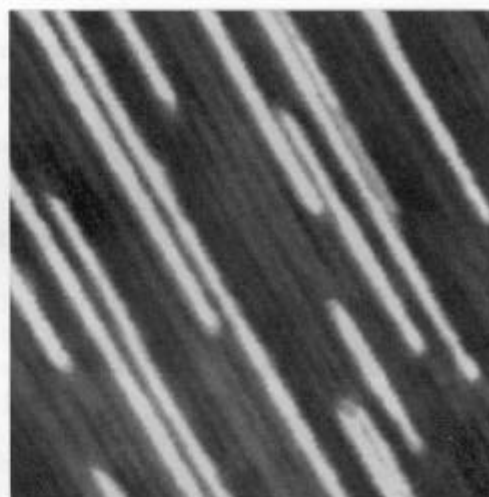


Fig. 3. A  $(400 \times 400) \text{ \AA}^2$  zoom-in from Fig. 1c, showing the Pd(110) morphology after hydrogen exposure of 300 min at  $2 \times 10^{-9}$  mbar.

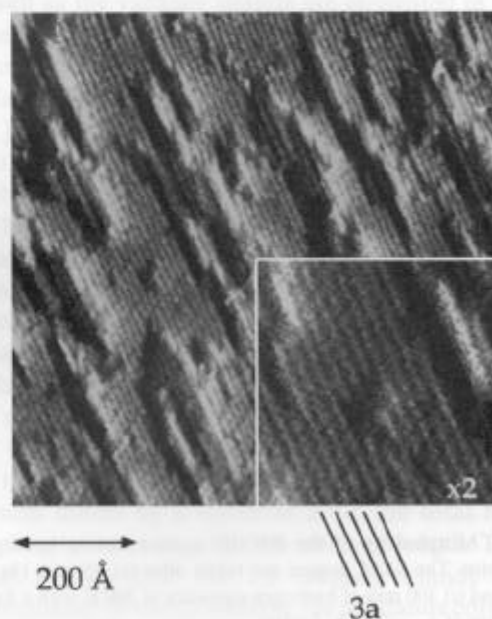


Fig. 4. Hydrogen induced  $(1 \times 3)$  reconstruction on the Pd(110) surface at 300 K after 400 min of hydrogen exposure at  $p_{H_2} = 2 \times 10^{-9}$  mbar.

involves again considerable mass transport. By comparing Fig. 4 with Fig. 3 and Fig. 1c it becomes evident that the final state is not just due to a lateral ordering of the missing rows but involves intra- and interlayer mass transport. While in the initial stage of the reconstruction only two layers are involved, the fully reconstructed  $(1 \times 3)$  phase is characterized by a rough morphology with at least 3 layers uncovered.

The hydrogen induced  $(1 \times 3)$  reconstruction was observed at steady state partial pressures of  $1 \times 10^{-9} \text{ mbar} \leq p_{\text{H}_2} \leq 5 \times 10^{-9} \text{ mbar}$ . Based on the adsorption isotherms measured by Conrad et al. and assuming a linearity between work function changes and hydrogen surface coverage  $\theta_{\text{H}}$ , the hydrogen induced  $(1 \times 3)$  surface phase exists at 300 K in the coverage range between  $0.3 \text{ ML} < \theta_{\text{H}} < 0.5 \text{ ML}$ . A monolayer here is defined by the maximum change in work function measured by Conrad et al. and is equivalent with the saturation coverage of hydrogen on the Pd(110) surface at  $T \geq 300 \text{ K}$ . Increasing the partial pressure to  $p_{\text{H}_2} = 5 \times 10^{-8} \text{ mbar}$  ( $\theta_{\text{H}} = 0.8 \text{ ML}$ ) results in a two phase regime which is shown in the STM image of Fig. 5. Patches of the  $(1 \times 3)$  reconstructed surface coexist besides large patches of a  $(1 \times 2)$  reconstructed surface. Approaching a hydrogen coverage of one monolayer a pure  $(1 \times 2)$  reconstruction is obtained. Following the already mentioned adsorption isotherms the hydrogen partial pressure at 300 K must be raised to  $p_{\text{H}_2} > 10^{-6} \text{ mbar}$ . Indeed Yoshinobu et al. observed a well ordered  $(1 \times 2)$  structure with an ambient pressure  $p_{\text{H}_2} = 5 \times 10^{-7} \text{ mbar}$  corresponding to  $\theta_{\text{H}} = 0.9 \text{ ML}$  [3].

Annealing experiments show that the hydrogen induced reconstructions are stable up to about 350 K. At this temperature the missing row reconstructions, the  $(1 \times 3)$  as well as the  $(1 \times 2)$  phase, are lifted and a nearly perfect  $(1 \times 1)$  surface structure is re-established. The temperature, where the lifting of the reconstruction takes place, coincides roughly with the maximum in the thermal desorption spectrum of bulk dissolved hydrogen [14]. We can, however, not unequivocally determine if desorbing hydrogen is the major destabilizing force of this transition, as Dhanak et al. have shown that the  $(1 \times 2)$  reconstructed Pd(110) surface is

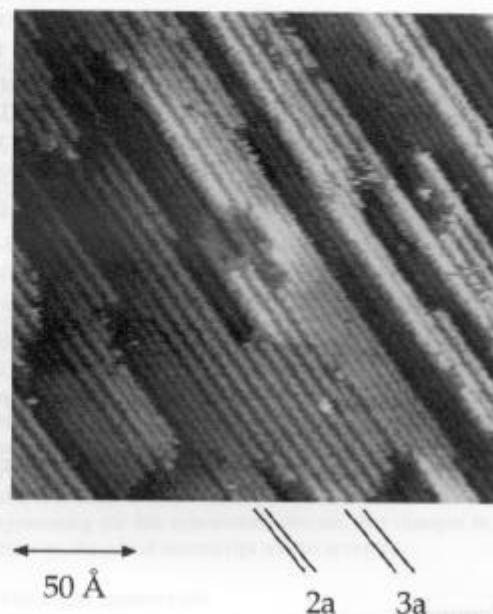


Fig. 5. Coexistence of the hydrogen induced  $(1 \times 3)$  and  $(1 \times 2)$  reconstruction on the Pd(110) surface at 300 K after 150 min of hydrogen exposure at  $p_{\text{H}_2} = 5 \times 10^{-8} \text{ mbar}$ .

stable up to 355 K and the  $(1 \times 3)$  reconstructed Pd(110) surface is stable up to 370 K both without any presence of adsorbed species [15].

The reconstruction scenario described here is similar to the hydrogen induced  $(1 \times 2)$  restructuring of the Ni(110) surface [4]. For this system Nielsen et al. studied the reconstruction kinetics by STM and evolved a combined missing-row/added-row reconstruction model. At low hydrogen coverages the authors also observed a low number of vacancy islands and Ni adatom islands both elongated along the closed packed  $[\bar{1}10]$  direction. Increasing the hydrogen coverage resulted in an increase of the amount of Ni rows which ended up in the regular arrangement of a  $(1 \times 2)$  reconstruction. No further ordered phase of the H/Ni(110) system was observed. The kicked out Ni atoms were found to nucleate at the surface to form monoatomic chains which had to be stabilized by adsorbed hydrogen. The missing rows and the added rows were observed at hydrogen coverages of 10% of a monolayer but reducing this coverage reduced also the Ni adatom density and the Ni surface relaxed into the original  $(1 \times 1)$

surface. For the H/Ni(110) system the restructuring of the surface is reversible and it depends on the adsorbed hydrogen coverage. This is at variance with the behavior of the H/Pd(110) system. The reconstructed Pd(110) surface is stable up to 350 K, the atoms nucleate at the surface to form adatom islands whose shape is kinetically determined by the temperature and the low Pd flux. It is not required to stabilize these Pd adatom islands by adsorbed hydrogen. Moreover, in the case of Pd(110) the adatoms do not take part in the main reconstruction process. This starts in the first Pd layer with the lateral ordering of the missing rows. Therefore the reconstruction process might be better described as being from the missing-row type.

#### 4. Summary

Our STM measurements reveal a hydrogen induced  $(1 \times 3)$  missing-row reconstruction at 300 K and hydrogen coverages between  $0.3 \text{ ML} < \theta_{\text{H}} < 0.5 \text{ ML}$ . With increasing hydrogen coverage a two phase regime with coexisting  $(1 \times 3)$  and  $(1 \times 2)$  reconstructions is passed before a pure  $(1 \times 2)$  phase is formed close to monolayer completion. Annealing experiments have shown that the reconstructed surfaces are stable up to 350 K. At this temperature the Pd(110) surface relaxes into the stable  $(1 \times 1)$  surface. The multi-phase behavior of the hydrogen induced reconstruction can be related to the small energy difference between the  $(1 \times n)$  missing row reconstructions of the transition metals [16]. The structure, thus, responds very sensibly to the charge re-distribution at the surface associated with the hydrogen coverage. A very

similar behavior has been observed for the Pt(110) surface [17]. The surface segregation of carbon impurities was found to change the  $(1 \times 2)$  missing-row phase of the clean surface into a  $(1 \times 3)$  phase by passing via a  $(1 \times 5)$  phase. The  $(1 \times 5)$  phase was identified to be a semi-ordered arrangement of  $(1 \times 2)$  and  $(1 \times 3)$  missing-row units; i.e. it corresponds to the ordered analog of the  $(1 \times 2)$ - $(1 \times 3)$  phase mixture seen for the H/Pd(110) system.

#### References

- [1] D.P. Woodruff, *J. Phys. Condens. Matter* 6 (1994) 6067.
- [2] H. Niehus, C. Hiller and G. Comsa, *Surf. Sci.* 173 (1986) L599.
- [3] J. Yoshinobu, H. Tanaka and M. Kawai, *Phys. Rev. B* 51 (1995) 4529.
- [4] L.P. Nielsen, F. Besenbacher, E. Laegsgaard and I. Stensgaard, *Phys. Rev. B* 44 (1991) 13156.
- [5] G. Kleinle, M. Skottke, V. Penka, G. Ertl, R.J. Behm and W. Moritz, *Surf. Sci.* 189/190 (1987) 177.
- [6] B.-S. Kang and K.-S. Sohn, *Physica B* 205 (1995) 163.
- [7] R.J. Behm, V. Penka, M.-G. Cattania, K. Christmann and G. Ertl, *J. Chem. Phys.* 78 (1983) 7486.
- [8] K.H. Rieder, M. Baumberger and W. Stocker, *Phys. Rev. Lett.* 51 (1983) 1799.
- [9] W. Eberhardt, S.G. Louie and E.W. Plummer, *Phys. Rev. B* 28 (1983) 465.
- [10] T. Engel and H. Kuipers, *Surf. Sci.* 90 (1979) 162.
- [11] E. Hahn, A. Fricke, H. Roeder and K. Kern, *Surf. Sci.* 297 (1993) 19.
- [12] J.P. Bucher, E. Hahn, P. Fernandez, C. Massobrio and K. Kern, *Europhys. Lett.* 27 (1994) 473.
- [13] N. Waelchli, E. Kampshoff and K. Kern, to be published.
- [14] H. Conrad, G. Ertl and E.E. Latta, *Surf. Sci.* 41 (1974) 435.
- [15] V.R. Dhanak, G. Comelli, G. Paolucci, K.C. Prince and R. Rosei, *Surf. Sci.* 260 (1992) L24.
- [16] M. Garofalo, E. Tosatti and F. Ercolessi, *Surf. Sci.* 188 (1987) 321.
- [17] I.K. Robinson, P. Eng and K. Kern, *Surf. Sci.*, in preparation.